Received: 8 January 2019 | Revised: 29 January 2019 | Accepted: 29 January 2019

DOI: 10.1002/pat.4579

RESEARCH ARTICLE

WILEY polymers advanced technologies

Electrospun electroactive nanofibers of gelatin-oligoaniline/Poly (vinyl alcohol) templates for architecting of cardiac tissue with on-demand drug release

Shahrokh Shojaie[1,2] | Mostafa Rostamian[3] | Ali Samadi[4] | Mohammad Amin Sabbagh Alvani[5] | Hossein Ali Khonakdar[6,7] | Vahabodin Goodarzi[8] | Roya Zarrintaj[9] | Morteza Servatan[10] | Azadeh Asefnejad[11] | Nafiseh Baheiraei[12] | Mohammad Reza Saeb[13,14,15]

[1] Department of Biomedical Engineering, Center Tehran Branch, Islamic Azad University, Tehran, Iran

[2] Stem Cells Research Center, Tissue Engineering and Regenerative Medicine Institute, Central Tehran Branch, Islamic Azad University, Tehran, Iran

[3] Department of Biomedical Engineering Faculty, South Tehran Branch, Islamic AZAD University, Tehran, Iran

[4] Polymer Engineering Department, Faculty of Engineering, Urmia University, Urmia, Iran

[5] School of Medicine, Shahid Beheshti University of Medical Sciences, Tehran, Iran

[6] Department of Polymer Processing, Iran Polymer and Petrochemical Institute, P.O. Box 14965-115, Tehran, Iran

[7] Leibniz Institute of Polymer Research Dresden, Hohe Straße 6, D-01069, Dresden, Germany

[8] Applied Biotechnology Research Center, Baqiyatallah University of Medical Sciences, Tehran, Iran

[9] Surgical Intensive Care Unit, Imam Khomeini Hospital, Urmia University of Medical Sciences, Urmia, Iran

[10] Department of Chemical Engineering, Urmia University of Technology, Urmia, Iran

[11] Department of Biomedical Engineering, Science and Research Branch, Islamic Azad University, Tehran, Iran

[12] Tissue Engineering and Applied Cell Sciences Division, Department of Hematology, Faculty of Medical Sciences, Tarbiat Modares University, Tehran, Iran

[13] Department of Resin and Additives, Institute for Color Science and Technology, Tehran, Iran

[14] Color and Polymer Research Center (CPRC), Amirkabir University of Technology, Tehran, Iran

[15] Advanced Materials Group, Iranian Color Society (ICS), Tehran, Iran

Correspondence
Vahabodin Goodarzi, PhD, Applied Biotechnology Research Center, Baqiyatallah University of Medical Sciences, P.O. Box 19945-546, Tehran, Iran.
Email: v.goodarzi@hotmail.com; v.goodarzi@bmsu.ac.ir

Mohammad Reza Saeb, PhD, Department of Resin and Additives, Institute for Color Science and Technology, P.O. Box 16765-654, Tehran, Iran.
Email: saeb-mr@icrc.ac.ir

In this study, grafted gelatin with oligoaniline (GelOA) was synthesized and then mixed with Poly (vinyl alcohol) (PVA). Several scaffolds with different ratio of PVA/GelOA were electrospun to fabricate electroactive scaffolds. GelOA was characterized using Fourier-transform infrared spectroscopy (FTIR); moreover, nanofiber properties were evaluated by differential scanning calorimetry (DSC), thermogravimetric analysis (TGA), and scanning electron microscope (SEM) analyses. Nanofibers diameter was decreased with aniline oligomer increment form 300 to 150 nm because of the hydrophobic nature of the aniline oligomer. Aniline oligomer electroactivity was studied using cyclic voltammetry, which exhibited two redox peaks at 0.4 and 0.6. Moreover, aniline oligomer enhancement resulted in melting point increasing from 220°C to 230°C because of the crystallinity increment. To assess the biocompatibility of nanofibers, cell viability and cell adhesion were tracked using mesenchymal stem cell (MSCs). It was revealed that the presence of aniline oligomer leads to enhancing the conductivity, thermal properties and lowering the degradation rate and drug release. Among of different scaffolds, sample with high content of GelOA shows better behavior in physical and biological properties. Accumulative drug releases under

applied electrical field at 40 minutes showed that the drug release for stimulated condition is about 33% more than the unapplied electrical field one.

KEYWORDS

conductive fiber, electroactive scaffold, gelatin, nanofiber, oligoaniline, tissue engineering

1 | INTRODUCTION

As mimicking tissue is a main goal in tissue engineering, various techniques have been developed to fabricate biomimic scaffolds such as salt leaching, 3D bioprinting, phase separation, casting, self-assembly, gelation, and electrospinning. Emulating extracellular matrix (ECM) as a dynamic cell niche by scaffolds can improve the tissue regeneration.[1] 3D scaffolds as porous media can structurally mimic the EMC, which can regulate the cell behavior. Architected scaffolds should exhibit the proper biocompatibility, cell proliferation, growth, adhesion, and differentiation. Designed scaffolds should also possess the high interconnected porosity with enormous specific surface area to provide the proper milieu with sufficient oxygen and nutrient permeation to support cell population and their distribution appropriately.[2-4]

Among different methods, nonwoven nanofiber mats can be fabricated by electrospinning technique as a simple and useful skill in which fibers diameter can be altered from microns to nanometers.[5] Various natural and synthetic polymers such as chitosan,[6,7] agarose,[8] starch,[9,10] Poly(lactic acid) PLA,[11] polycaprolactone (PCL)[12] have been used to fabricate the electrospun nanofibers.[13] In this regards, wide ranges of properties such as enriched mechanical/thermal properties,[14] conductivity[15] and porosity[16] can be achieved by the selection of proper materials. Nanofibers along with high surface to volume ratio and adjustable mechanical, porous topological features, low cost, tunable flexibility, and strength as an applicable technique have been utilized in various applications with on large scale[17] such as removal,[18] wearable strain sensors,[19] high temperature detector,[20] and fuel cells,[21] exchange membrane[22] moreover, nanofibers can provide a proper milieu for cellular activities.[23]

Gelatin is one of the most promising biocompatible materials, which are fabricated form collagen hydrolysis as a major protein of connective tissue. This material is more affordable in comparison with collagen containing Arg-Gly-Asp (RGD)-like sequences of amino-acids, which enhance cell proliferation, adhesion, and migration. However, gelatin lacks suitable mechanical properties and rapid degradation rate because of collagenase action.[24,25] To overcome such problem, gelatin has been blended with other polymers to enhance its properties. Poly (vinyl alcohol) (PVA) as a semicrystalline synthetic, hydrophilic polymer with proper mechanical, chemical, and thermal properties has been widely used for in tissue engineering. PVA properties depend on its polymerization and hydrolysis degree.[26,27] It was reported that the oxidized level of the PVA affects the nerve regeneration. Oxidized PVA (OxPVA) along with axon regeneration exhibited the proper elasticity and manipulation. OxPVA promoted the myelination and axon density.[28] In comparison with other biomaterials, PVA shows an excellent effects in biomedical application like to ECM. For example, epoxy materials due to existing of toxic low molecular weight can resulted in cell toxicity.[29-33] Moreover, PVA has hydrophilic property and dissolve in water, but epoxy families are soluble in organic solvent.[34-36] Therefore, this result is powerful warranter in biocompatibility and biodegradability of PVA. In comparison with polyolefin families,[37-41] hydro-catalytic degradation rate of PVA can be tuned to targeted tissue. PVA exhibits a proper hydrophilicity role in cell attachment while this property in polydimethylsiloxane (PDMS) and other thermoplastic polymers are very weak.[42-44] Various types of polymeric scaffolds can be generated by many methods. Electrospinning is a powerful technique in manufacturing of numerous scaffolds. In this method porosity, size of fibers and also mechanical properties can be easily controlled by operational factors.[45] Production of biodegradable nanofibers can be effective in generation of high performance scaffolds. On the other hand, doped PVA with various nanoparticle and other conductive materials developed a new class of materials with unique features and high application in many fields such as photocatalytic activity, anticorrosive, and hyperthermia.[46-49] Therefore, modification of PVA is performed based on its application and properties. A main method for improving of PVA properties is blending with other polymeric materials. In this regard, some related researches have been reported in Table 1.

In recent decades, requirement to new materials is very necessary due to progress in many scientific fields. In among of various materials,

TABLE 1 Some related researches about of properties and applications of Poly (vinyl alcohol) (PVA)

Material	Application	Properties	Ref
Graphene oxide-PVA	Enzyme immobilization	Three-dimensional network structure, more binding sites, high stability	50
Polyvinyl alcohol-chitosan	Antioxidant	Freezing–thawing, enhanced thermal and mechanical performances	51
Chitosan/polyvinyl alcohol/zeolite	Membrane	Increased tensile strength, high adsorption rate	52
Starch-polyvinyl alcohol	Packaging	Biodegradable, high tensile strength, controlled permeability	53
ZnO/polyvinyl alcohol/chitosan	Wound dressing	Low water vapor transmission rate, low absorption of wound fluids	54

Abbreviation: PVA: Poly (vinyl alcohol)

conductive materials are very interested. Conductive materials such as carbon nanotube,[55] graphene,[56] graphene oxide,[57] polyaniline,[58] polypyrrole,[59] and metal[60,61] have been widely used in various applications including corrosion,[62] electromagnetic interference (EMI) fielding,[63] polluted water treatment,[64] catalysis,[65] battery,[66,67] CO_2 reduction,[68] structural composites,[69,70] and medicine.[71-73]

It has been demonstrated that the conductive substrates enhance the cellular activity with and without electrical stimulation. Different electroactive moieties including gold, carbon nano tubes, graphene, and conductive polymers have been utilized in tissue engineering.[74] Conductive polymers like polyaniline, polypyrrole, and polythiophene have attracted intense attentions because of their adjustable properties and unique behavior. Cellular/protein attachment can be altered by adjusting the redox state of the conductive polymer. Among conductive polymers, polyaniline due to the ease of synthesis, tunable conductivity, and affordable cost has been widely used for biomedical applications.[75] However, in vivo usage of conductive materials due to their nondegradability/poor degradability is restricted.[76] Due to such restriction, new emerging conductive oligomers have been attracted significant attentions in tissue engineering field. Oligoaniline-based conductive bio materials have been proposed to provide the proper biocompatibility and conductivity along with proper degradation rate.[77]

Mohammadi et al synthesized polyaniline-based nanofibers for cardiac tissue engineering. It was demonstrated that the conductive substrate enhance the induced pluripotent stem cell differentiation to myocardium cell in comparison with nonconductive substrate.[78,79] Also, it has been reported that the agarose-aniline pentamer enhances the neural regeneration.[80] Oligoaniline-based biomaterial degradation rate can be tuned in comparison with polyaniline. Aniline oligomers can be used to adjust the scaffold properties such as mechanical feature, hydrophilicity, and degradation rate and drug release.[81] Atoufi et al synthesized alginate-aniline tetramer scaffold, which exhibited the shape-memory behavior, adjustable swelling, and degradation rate.[82] Gelatin-aniline oligomer hydrogel was synthesized with on-demand electro-responsive properties in which the loaded drug was released with arbitrary pattern.[83] Chen et al fabricated PLA/polyaniline nanofibers for bone regeneration. It was reported that the nanofibrous structure resulted in proper cytocompatibility, calcium mineralization, proliferation, and osteogenic differentiation.[84] Fernandes et al fabricated poly lysine/polyaniline nanofibers for cardiac regeneration. Electrical stimulation using such platform enhanced the cellular activity.[85] Cellular behavior can be regulated using various stimulation methods such as electrical stimulation, hydrodynamic pressure, and culture media,[79,86,87] which it has been demonstrated that the electrical stimulation as a unique technique enhances the cellular activity.[88] Baheiraei et al fabricated electroactive scaffolds composed of polyurethane/aniline pentamer, blended with PCL as cardiac patch. Synthesized samples exhibited electrical conductivity

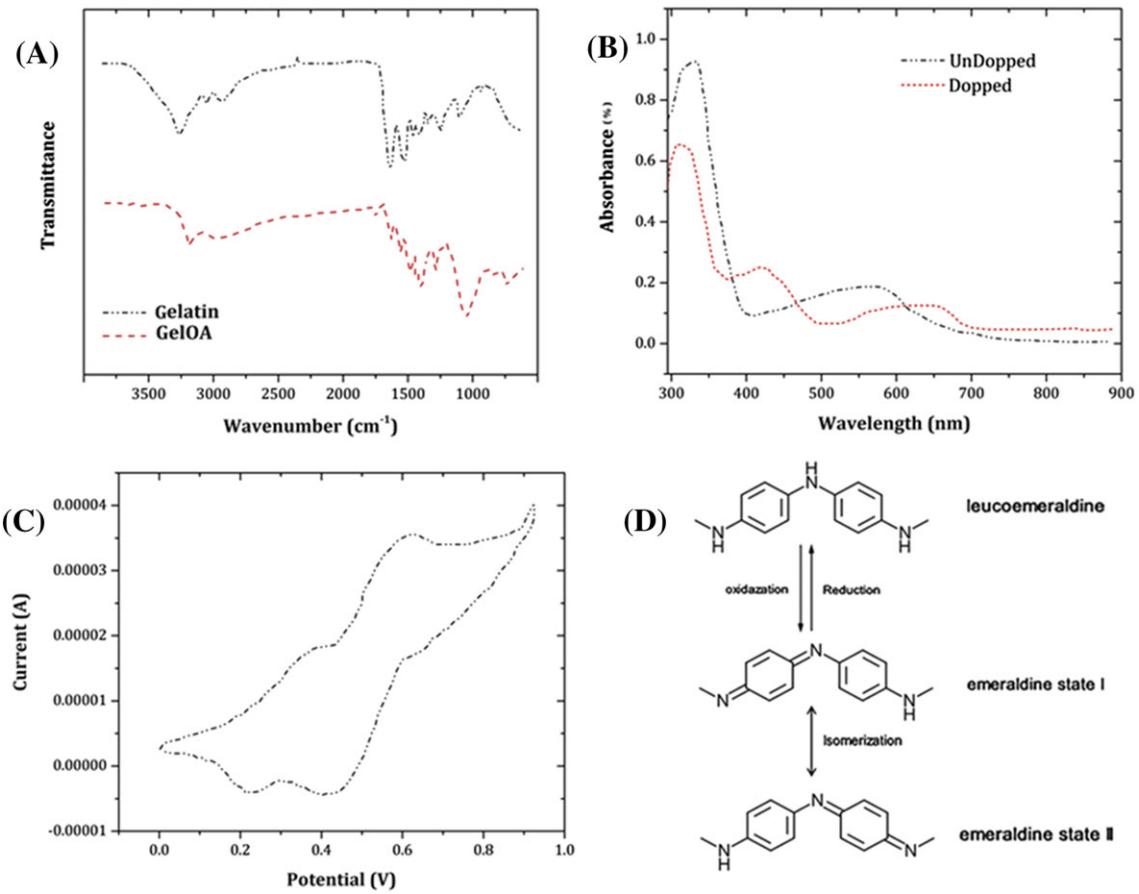

FIGURE 1 (A) Fourier-transform infrared spectroscopy (FTIR) peaks of sample (B) UV–Vis of doped and undoped samples (C) cyclic voltammetry of sample (D) oxidation/reduction state of the oligoaniline [Colour figure can be viewed at wileyonlinelibrary.com]

in semiconductor range (~10^{-5} S/cm) and upregulated neonatal cardiomyocytes genes compared with that on nonconductive substrate.[89] In another study, the authors demonstrated that polyurethane/siloxane films containing aniline tetramer, as an electroactive structures, are compatible with proliferation of C2C12 and have the potential to improve formation of myotubes even without external electrical stimulation.[90]

In our previous study,[83] conductive hydrogel based on gelatin was synthesized, and the optimum percentage of the aniline oligomer was determined to achieve the best biocompatibility. Here, in this study, conductive nanofibers based on gelatin-oligoaniline/PVA were synthesized, and well-defined scaffolds were manufactured by electrospinning technique. We hypothesized that enhanced electroactive role of the architected scaffolds can be effective on cellular function. Furthermore, we extensively studied general and cell behavior including conductivity, electroactivity, thermal behavior, morphology, and biocompatibility on the developed gelatin-oligoaniline/PVA scaffolds.

2 | MATERIALS AND EXPERIMETALS

2.1 | Materials

Gelatin, PVA, N-Phenyl-p-phenylenediamine, glutaraldehyde, and p-phenylenediamine were purchased from Sigma-Aldrich Co., Germany. Succinic anhydride, ammonium peroxidisulfate ($(NH_4)_2S_2O_8$), and solvents were received from Merck Company (Germany). All materials were utilized without any purification.

2.2 | Gelatin-aniline oligomer synthesis and spinning solutions preparation

To achieve the carboxylic capped aniline oligomer, the same molar of succinic anhydride and N-Phenyl-p-phenylenediamine were dissolved in dichloromethane being reacted at 50°C for 48 hours. After that, it was added to gelatin solution, and ammonium peroxidisulfate was added dropwisely to the mixture to achieve the gelatin with oligoaniline (GelOA).

PVA was dissolved in water for 24 hours, then, solution was stirred at 50°C for 4 hours to achieve the 15 wt.% aqueous homogeneous solution. Different ratios of PVA/GelOA (1:10, 3:10, and 5:10) were prepared, which were designated G1, G2, G3, respectively. Spinning solution was stirred at room temperature overnight. 10 cc syringes with 0.4 mm inner diameter needle were utilized for electrospinning. The flow rate, needle-collector distance, and applied voltage were 50 μl $minutes^{-1}$, 15 cm, and 15 kV, respectively. After electrospinning, nanofibers were exposed to the glutaraldehyde vapors overnights. Finally, electrospun nanofibers were rinsed using deionized and then were rinsed using PBS to remove the nonreacted residual.

2.3 | Characterization

The synthesized structures were characterized using Fourier-transform infrared spectroscopy (FTIR) apparatus using Bruker instrument (Germany) form 4000 to 600 cm^{-1} wavelength at room temperature. UV–Vis was utilized to determine the oligoaniline transition state using Shimadzu Multispec spectrophotometer (Japan).

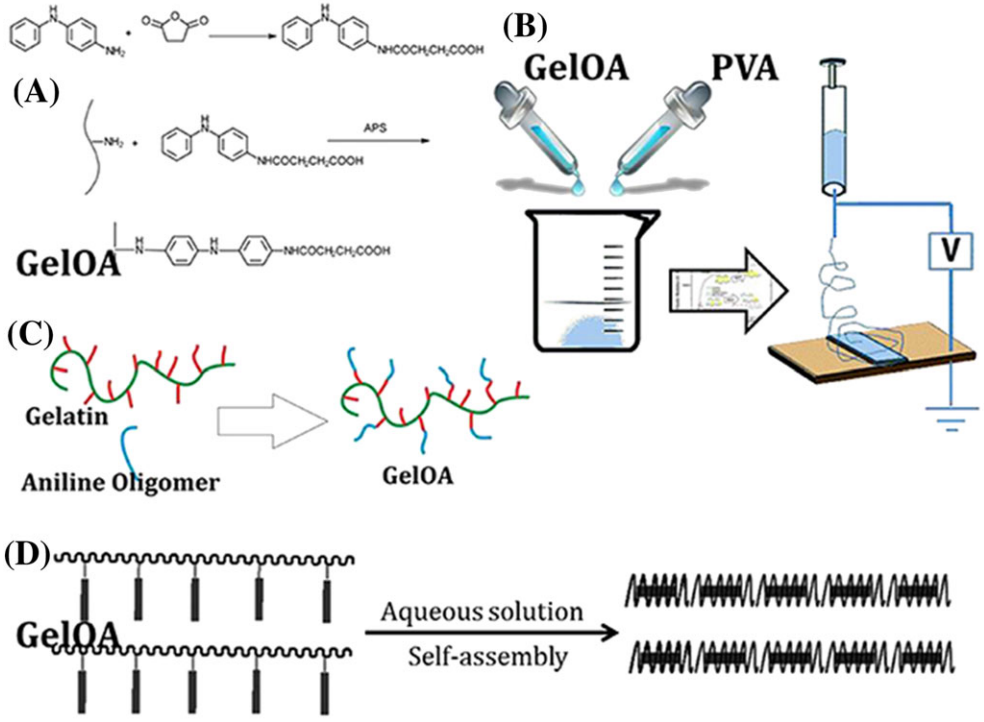

FIGURE 2 (A) Synthesis route of gelatin with oligoaniline (GelOA) (B) electrospinning method (C) schematic of GelOA (D) self-assembly of GelOA [Colour figure can be viewed at wileyonlinelibrary.com]

2.4 | Conductivity measurement and electroactivity evaluation

Four-probe method was utilized to determine the samples conductivity using the following Equation 1:

$$\sigma = \left(\frac{1}{R}\right) \times \left(\frac{d}{S}\right), \quad (1)$$

where S, d, R, and σ are surface area, thickness, resistance, and conductivity. Cyclic voltammetry (C.V.) and UV–Vis were utilized to assess the electroactivity using micro auto lab and UV spectroscopy instrument, respectively. Doped and undoped transition states of oligoaniline were studied in the ranges of 260-1000 nm. To evaluate the C.V. working, reference and counter electrodes were carbon paste, Ag/AgCl and platinum, respectively along with scan rate of 50 mVs^{-1}.

2.5 | Thermal behavior analysis

Thermal behavior of samples was studied using thermogravity analysis (TGA) and differential scanning calorimetry (DSC). DSC was performed under nitrogen atmosphere from 0°C to 250°C at 10°C $minutes^{-1}$. TGA was utilized to investigate the thermal stability under nitrogen atmosphere from ambient temperature to 800°C at 10°C $minutes^{-1}$ heating rate.

2.6 | Morphology analysis

Nanofibers morphology was studied using Hitachi (Japan) scanning electronic microscopy (SEM). To prepare for SEM imaging, the nanofibers were sputter coated using gold sprouting. Nanofibers diameter and their distribution were also studied using Image J software.

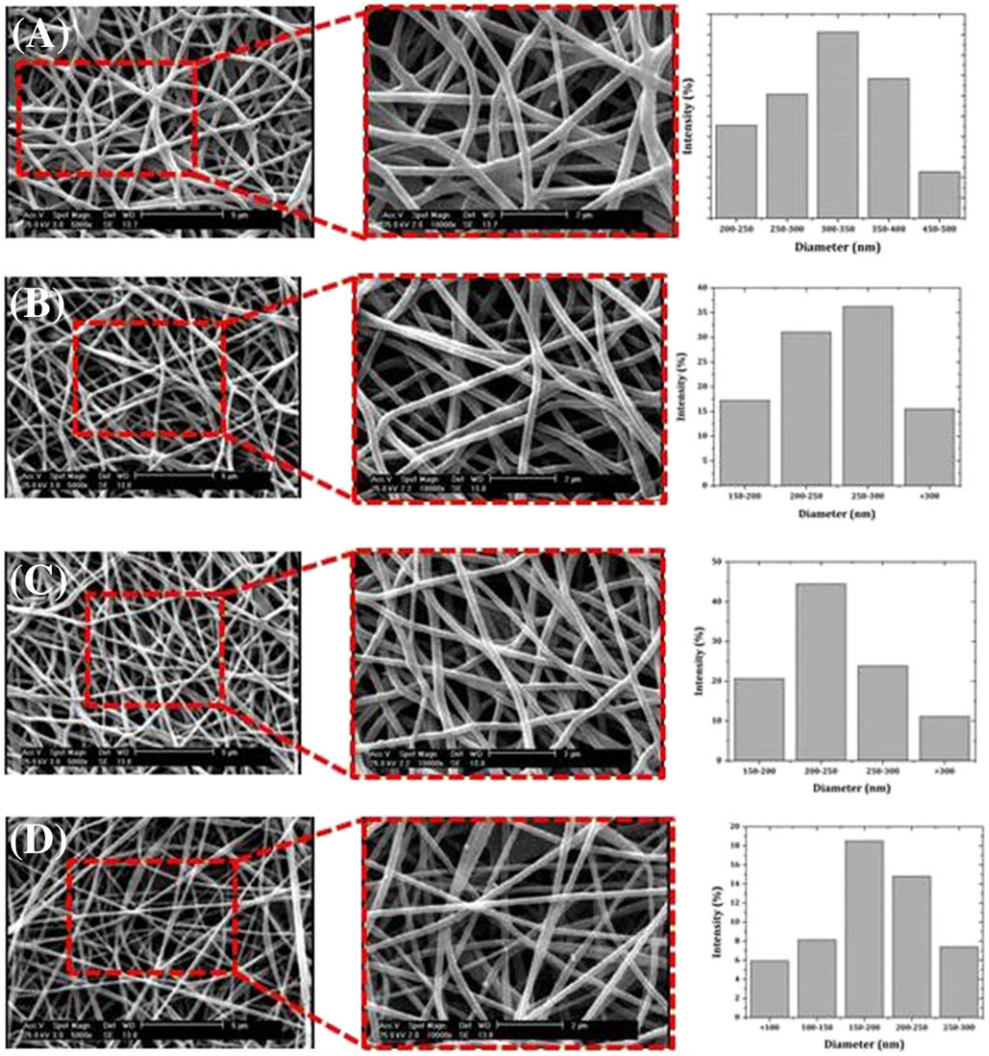

FIGURE 3 (A) Poly (vinyl alcohol) (PVA) nanofibers (B) G1 nanofibers (C) G2 nanofibers (D) G3 nanofibers [Colour figure can be viewed at wileyonlinelibrary.com]

2.7 | In vitro biodegradation

To assess the degradation rate, nanofibers were immersed in PBS being incubated at 37°C. At specific time intervals, nanofibers were removed from PBS, washed with deionized water, and dried. After that, samples were weighted to calculate the degradation rate (%) using Equation 2. To assess the degradation rate, sterilized scaffolds were dried and weighed before being placed in PBS (pH = 7.4) at 37°C. At different intervals, samples were taken out, washed with DI water, and dried in a vacuum. The percentage of weight loss was calculated as

$$Weight \quad loss(\%) = \frac{W_1 - W_2}{W_1} \times 100, \tag{2}$$

where W_1 and W_2 are the weights of the samples before and after degradation, respectively.

2.8 | Drug release behavior

Drug release behavior from nanofibers was studied using dexamethasone (DX) from corticosteroid family member with immunesuppressant and anti-inflammatory feature. In this regards, determined amount of DX was poured in spinning solution and was electrospun. To evaluate the release pattern, nanofibers were soaked in PBS to determine release rate. The release amount of drug was determined by UV–Vis spec at 237 nm.

2.9 | Biocompatibility evaluation

To evaluate the biocompatibility, mesenchymal stem cells (MSCs) (received from Pastor Institute of Iran) were cultured on nanofibers, and MTT assay was performed. In this regards, samples were sterilized using UV and ethanol. Samples were immersed in culture medium (Dulbecco's Modified Eagle's Medium) overnight. Following that, samples were rinsed by PBS, and MSCs were seeded on them; after that, cell viability was assessed. Cytocompatibility evaluation was performed using 3-[4,5-dimethylthiazol-2-yl]-2,5-diphenyltetrazolium bromide (MTT, Sigma) colorimetric assay after 1, 3, and 5 days post seeding. Before cell culture, sterilized scaffolds were incubated with complete medium of Dulbecco's Modified Eagle's Medium F12 (DMEM F12; Gibco) with 100 IU/mL penicillin, 100 IU/mL streptomycin, and 10% fetal bovine serum (FBS; Gibco) over night. Then, 3 × 104 cells were seeded over scaffolds in 96 well culture plates and incubated at 37°C. At each interval, 150 µL solution containing a 5:1 ratio of media and MTT (5 mg/mL in PBS) was added to each well for 3 hours. The medium was then removed, and the formazan precipitates were dissolved in dimethyl sulfoxide (DMSO, Gibco). The optical absorbance at 570 nm was measured using a microplate reader.

The morphology of the cultured cells was evaluated by SEM after 48 hours. Cells were fixed in 2.5% glutaraldehyde and dehydrated with graded ethanol solutions (10%, 30%, 70%, 90%, and 100%) before being coated with gold and investigated by SEM.

2.10 | Statistical analysis

One way analysis of variance (ANOVA) was used for significant difference ($P < 0.05$) of deviation among parameters.

3 | RESULTS AND DISCUSSIONS

Succinic anhydride was used to cap the oligoaniline to hinder the further reactions. Oligoaniline carboxylic capped was reacted with gelatin

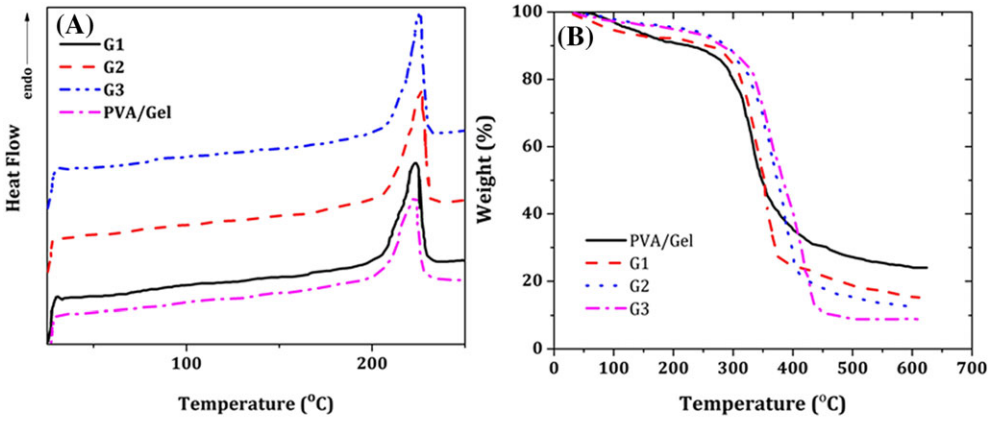

(C)

	T_m	ΔH_f	X_c
PVA/Gel	223.4	88.81	64.15
G1	224.7	91.7	65.38
G2	225.5	92.1	66.41
G3	226.1	94.41	68.1

FIGURE 4 (A) Differential scanning calorimetry (DSC) and (B) thermogravimetric analysis (TGA) diagram of samples (C) thermal analysis of samples [Colour figure can be viewed at wileyonlinelibrary.com]

amine groups using ammonium peroxidisulfate. To assess the chemical structure of the GelOA, FTIR spectrum was utilized, which is presented in Figure 1A in which reveals the peaks at 1236 and 1520 cm^{-1} is related to the N—H out-of-plane bending bond of amine types III and II. C=O stretching vibration is presented around 1630 cm^{-1}, and C—H stretching vibration alkyl groups appear around 2935 cm^{-1}. Characteristic peaks of GelOA is presented around 1496 cm^{-1} and 1580 cm^{-1}, which are attributed to the benzenoid diamine ring (—N—B—N—) and quinine diimine ring (—N=Q=N—). Figure 1B depicts two transition peak at 334 nm relate to the π-π* transition and peak at 584 nm ascribe to the benzenoid-to-quinoid excitonic transition (πB-πQ). Solvatochromism effect was observed after doping GelOA using camphor sulfonic acid, which peaks was shifted to 320 and 420 nm.

Figure 1C illustrates that the electroactivity the aniline oligomer, which fluctuates between reduction and oxidation states. CV test exhibits two reversible peaks at 0.4 relate to transition from leucoemeraldine to emeraldine state and 0.6 ascribe to emeraldine state I to emeraldine state II (Figure 1D). Steric hindrances and short chain segments caused to restrict in complete redox state transition and two state of redox state were observed. Four probe method was used to evaluate the nanofibers conductivity. It was revealed that the GelOA content increment resulted in conductivity increasing. DC conductivity measurements of G1, G2, and G3 were about 2.1×10^{-6}, 8.4×10^{-6}, and 3.6×10^{-5} (S/m), respectively, which are adequate value (human body voltage is about 1 ~ 5 mV) for bioelectrical signal transfer and tissue regeneration.[91]

The synthesis steps from preparing of GelOA component and formulating of PVA/GelOA solution for electrospinning method are schematically shown in Figure 2.

SEM images (Figure 3) of nanofibers reveal that the oligoaniline addition decreases the nanofibers diameter. Fiber diameter of PVA, G1, G2, and G3 were around 342, 283, 228, and 195 nm, respectively. Oligoaniline presence in polymeric chain segment resulted in hydrophobicity of nanofibers (Figure 3B, Figure 3C, and Figure 3D). In aqueous media, oligoaniline segments tended to encapsulate

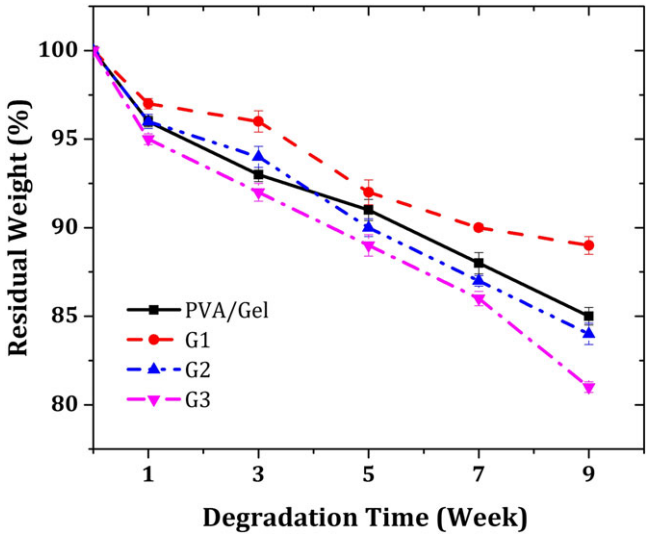

FIGURE 5 Degradation kinetics of nanofibers [Colour figure can be viewed at wileyonlinelibrary.com]

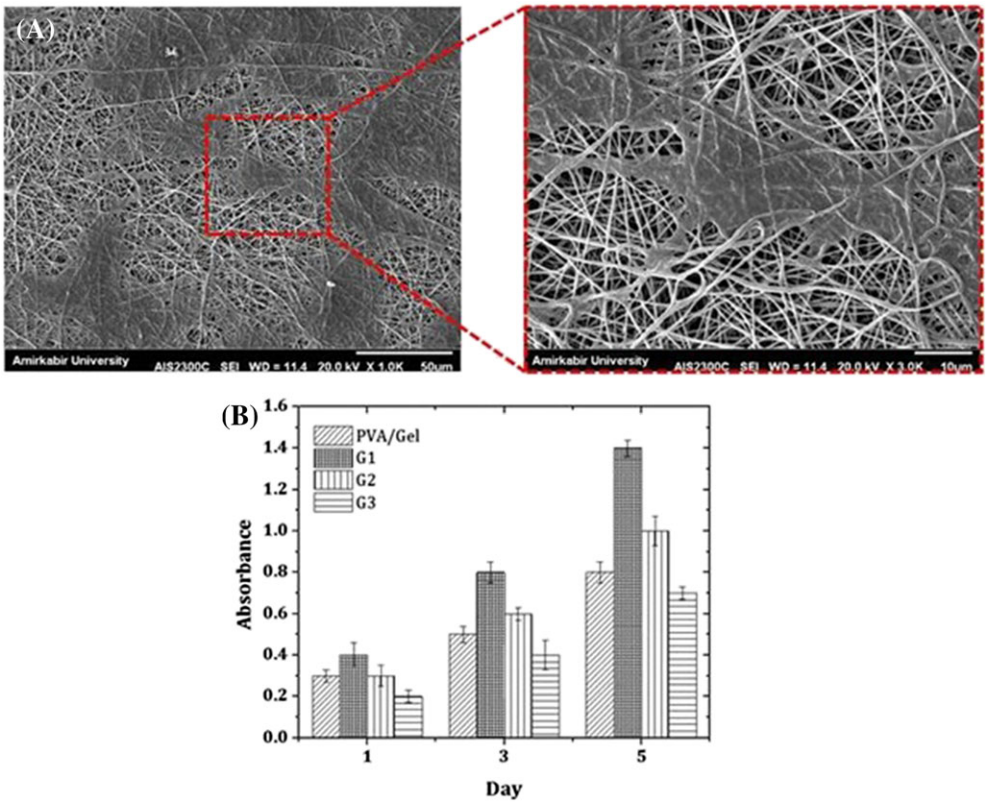

FIGURE 6 (A) Cell adhesion on G1, (B) cell viability of nanofibers [Colour figure can be viewed at wileyonlinelibrary.com]

spontaneously within the soft gelatin chains, and nanofibers diameters were decreased. Aniline oligomer presence enhanced the solution hydrophobicity, and the solution viscosity was decreased. Viscosity decrement resulted in fiber diameter decrement.[92]

Thermal behavior of nanofibers was studied by TGA and DSC (Figure 4). DSC results revealed that the oligoaniline enhanced the crystallinity and melting temperature of the nanofibers. Oligoaniline acted as a nucleating agent and enhance the crystallinity, and therefore, melting temperature was increased. TGA was utilized to study the thermal stability of the nanofibers. Oligoaniline presence in polymer chains enhances the thermal stability because of its rigid structure. Three steps are observed in TGA curves, which first step before 250°C is attributed to the solvent and moisture volatilization trapping within mats, the second step between 200°C and 400°C is related to the gelatin/PVA degradation, and final step is related to the oligoaniline degradation and carbonization.[93]

Figure 5 exhibits the degradation rate of the nanofibers degradation rate. It is revealed that the nanofibers diameter and hydrophobicity are effective factors in degradation process. Accordingly, all samples obeyed the same degradation kinetics. All samples obeyed the same degradation kinetics. Lower diameter of nanofibers resulted in higher surface area of nanofibers exposes with aqueous media; hence, degradation rate was enhanced with lowering the nanofibers diameter. On the other hand, oligoaniline presence in nanofibers structure hindered the aqueous media penetration and repels the aquatic milieu. In this regards, G1 represented the lower degradation rate. Fibers degradation can be attributed to the polymer chain and hydrolytic chain cleavage relaxation in aquatic milieu.[94]

The cell adhesion on surface of selected nanofiber matt (G1) and MTT assay were investigated and presented in Figure 6. Cell attachment of G1 sample is depicted in Figure 6A and 6B at two magnifications. Notably, attached cells on surface of scaffolds can be clearly seen. This observation advent in electroactive gelatin-oligoaniline pair of scaffolds. This property extensively increases rate of ions exchange, and cells grow more. MTT assay was utilized to evaluate metabolic activity of cells growing on prepared platforms and obtained results showed in Figure 6C. It was demonstrated that the G1 had the highest biocompatibility. Oligoaniline endowed the conductivity to the nanofibers, which enhanced the cellular activity due to the electroactivity of substrate causing to chemical and energy exchange between platform and cells. In this regards, MSCs proliferation was enhanced on conductive nanofiber rather than nonconductive one. It was speculated that the increment of oligoaniline concentration in nanofibers caused to cellular toxicity, and cellular growth was hindered. Hence, oligoaniline content should be optimized, which G1 exhibited the best performance.

Dynamic drug release from nonconductive and conductive nanofibers (NF), stimulated and passive release and mechanism of drug release of electroactive scaffold were presented in Figure 7.

Dynamic drug release from scaffolds with nonconductive and conductive NF without applied electrical field was presented in Figure 7A. Release pattern of DX from nonconductive NF was higher than conductive NF. This can be due to the presence of grafted oligoanilines on gelatin backbone because its hydrophobicity increases. Therefore, resistance to water penetration in conductive NF enhanced. This finding is a critical feature in electroactive scaffolds for modulating of drug release. Such method can be used as an on-demand drug release with desired pattern.[95,96]

Drug release from electroactive scaffold with and without electrical field was depicted in Figure 7B. As can be realized from this figure, applied electrical field (stimulated) has substantially effect on release profile. By comparing between cumulative drug releases values of passive and stimulated conditions showed that the drug release at 40 minutes for stimulated condition is about 33% more than the passive one. As expected, drug accumulation centers inside of electroactive scaffold destroyed under applied electrical field.

For better realizing about drug release from electroactive scaffold under applied electrical field, a clear mechanism was presented in Figure 7C.

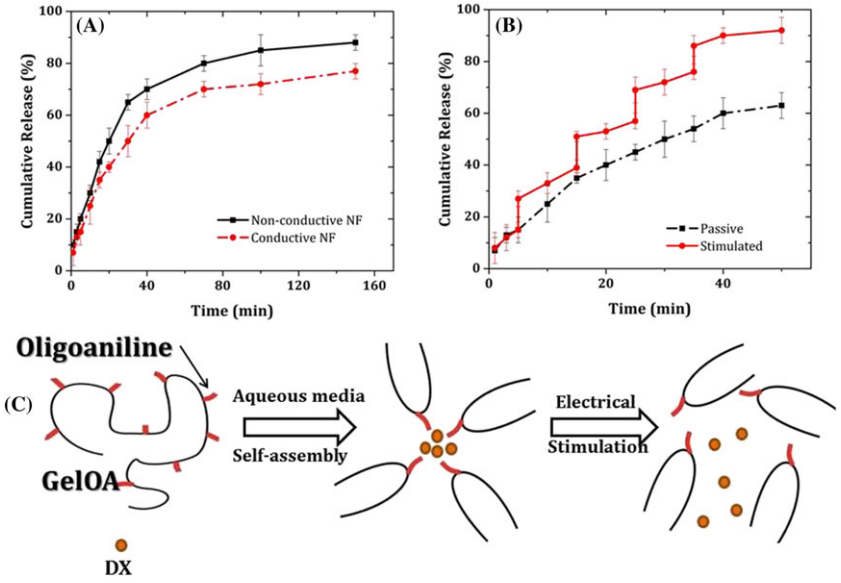

FIGURE 7 (A) Drug release from nonconductive and conductive nanofibers (NF), (B) stimulated and passive release (C) mechanism of drug release [Colour figure can be viewed at wileyonlinelibrary.com]

4 | CONCLUSION

Mimicking the ECM behavior as a cell niche is a challenging task in tissue engineering. Nanofibrous conductive scaffolds can recapitulate the ECM milieu. In this regards, conductive polymer based on gelatin and oligoaniline was synthesized after that it was electrospun to achieve the nanofibrous structure. FTIR was utilized to characterize the nanofibers characteristics. DSC and TGA were used to evaluate the thermal behavior of the samples. Oligoaniline presence endows the conductivity to the nanofibers along with thermal stability enhancement. Nanofibers diameters were reduced with increasing the oligoaniline content because of the oligoaniline hydrophobicity and solution viscosity decrement. Nanofibers diameter decrement causes to higher exposure with aquatic media, which resulted in increasing degradation rate. Oligoaniline content should be optimized to achieve the best content to achieve the proper conductivity along with higher compatibility, which G1 exhibited the best biocompatibility. Oligoaniline presence in nanofibers hindered the drug release rate because of the entrapment of DX within oligoaniline. On-demand drug release can be achieved by electrical stimulation. Conductive nanofibers because of the ECM-like structure can be used potentially as a wound dressing, neural conduit, and cardiac patch. Such platform can pave a way to design novel scaffolds to emulate the tissue properties.

ORCID

Vahabodin Goodarzi https://orcid.org/0000-0002-7295-5434

REFERENCES

1. Nilforoushzadeh MA, Zare M, Zarrintaj P, et al. Engineering the niche for hair regeneration–a critical review. *Nanomed Nanotechnol Biol Med*. 2019;1:70-85.
2. Bakhshandeh B, Zarrintaj P, Oftadeh MO, et al. Tissue engineering; strategies, tissues, and biomaterials. *Biotechnol Genet Eng Rev*. 2017;33(2):144-172.
3. Zarrintaj P, Saeb MR, Ramakrishna S, Mozafari M. Biomaterials selection for neuroprosthetics. *Curr Opin Biomed Eng*. 2018;6:99-109.
4. Zarrintaj P, Ahmadi Z, Saeb MR, Mozafari M. Poloxamer-based stimuli-responsive biomaterials. *Materials Today: Proc*. 2018;5(7):15516-15523.
5. Zarrintaj P, Moghaddam AS, Manouchehri S, et al. Can regenerative medicine and nanotechnology combine to heal wounds? The search for the ideal wound dressing. *Nanomedicine*. 2017;12(19):2403-2422.
6. Amirabad LM, Jonoobi M, Mousavi NS, Oksman K, Kaboorani A, Yousefi H. Improved antifungal activity and stability of chitosan nanofibers using cellulose nanocrystal on banknote papers. *Carbohydr Polym*. 2018;189:229-237.
7. Mohebbi S, Nezhad M, Zarrintaj P, et al. Chitosan in biomedical engineering: a critical review. *Curr Stem Cell Res Ther*. 2018;13.
8. Zarrintaj P, Manouchehri S, Ahmadi Z, et al. Agarose-based biomaterials for tissue engineering. *Carbohydr Polym*. 2018;187:66-84.
9. Yarahmadi E, Didehban K, Sari MG, et al. Development and curing potential of epoxy/starch-functionalized graphene oxide nanocomposite coatings. *Prog Org Coat*. 2018;119:194-202.
10. Sari MG, Vahabi H, Gabrion X, et al. An attempt to mechanistically explain the viscoelastic behavior of transparent epoxy/starch-modified ZnO nanocomposite coatings. *Prog Org Coat*. 2018;119:171-182.
11. Laoutid F, Vahabi H, Shabanian M, Aryanasab F, Zarrintaj P, Saeb M. A new direction in design of bio-based flame retardants for poly (lactic acid). *Fire Mater*. 2018;42(8):914-924.
12. Low K, Chartuprayoon N, Echeverria C, et al. Polyaniline/poly (ε-caprolactone) composite electrospun nanofiber-based gas sensors: optimization of sensing properties by dopants and doping concentration. *Nanotechnology*. 2014;25(11):115501.
13. Lu Y, Huang J, Yu G, et al. Coaxial electrospun fibers: applications in drug delivery and tissue engineering. *Wiley Interdiscip Rev Nanomed Nanobiotechnol*. 2016;8(5):654-677.
14. Gu J, Li Y, Liang C, et al. Synchronously improved dielectric and mechanical properties of wave-transparent laminated composites combined with outstanding thermal stability by incorporating iysozyme/POSS functionalized PBO fibers. *J Mater Chem C*. 2018;6(28):7652-7660.
15. Wang C, He Z, Xie X, et al. Controllable cross-linking anion exchange membranes with excellent mechanical and thermal properties. *Macromol Mater Eng*. 2018;303(3):1700462.
16. Guo Y, Xu G, Yang X, et al. Significantly enhanced and precisely modeled thermal conductivity in polyimide nanocomposites with chemically modified graphene via in situ polymerization and electrospinning-hot press technology. *J Mater Chem C*. 2018;6(12):3004-3015.
17. Zhang L, Yu W, Han C, et al. Large scaled synthesis of heterostructured electrospun TiO2/SnO2 nanofibers with an enhanced photocatalytic activity. *J Electrochem Soc*. 2017;164(9):H651-H656.
18. Huang J, Cao Y, Shao Q, Peng X, Guo Z. Magnetic nanocarbon adsorbents with enhanced hexavalent chromium removal: morphology dependence of fibrillar vs particulate structures. *Ind Eng Chem Res*. 2017;56(38):10689-10701.
19. Li Y, Zhou B, Zheng G, et al. Continuously prepared highly conductive and stretchable SWNT/MWNT synergistically composited electrospun thermoplastic polyurethane yarns for wearable sensing. *J Mater Chem C*. 2018;6(9):2258-2269.
20. Guan X, Zheng G, Dai K, et al. Carbon nanotubes-adsorbed electrospun PA66 nanofiber bundles with improved conductivity and robust flexibility. *ACS Appl Mater Interfaces*. 2016;8(22):14150-14159.
21. Wang C, Mo B, He Z, et al. Crosslinked norbornene copolymer anion exchange membrane for fuel cells. *J Membr Sci*. 2018;556:118-125.
22. Wang C, Mo B, He Z, et al. Hydroxide ions transportation in polynorbornene anion exchange membrane. *Polymer*. 2018;138:363-368.
23. Alhosseini SN, Moztarzadeh F, Mozafari M, et al. Synthesis and characterization of electrospun polyvinyl alcohol nanofibrous scaffolds modified by blending with chitosan for neural tissue engineering. *Int J Nanomedicine*. 2012;7:25.
24. Kazemi M, Azami M, Johari B, et al. Bone regeneration in rat using a gelatin/bioactive glass nanocomposite scaffold along with endothelial cells (HUVEC s). *Int J Appl Ceram Technol*. 2018;15(6):1427-1438.
25. Ghorbani F, Nojehdehyan H, Zamanian A, Gholipourmalekabadi M, Mozafari M. Synthesis, physico-chemical characteristics and cellular behavior of poly (lactic-co-glycolic acid)/gelatin nanofibrous scaffolds for engineering soft connective tissues. *Adv. Mater Lett*. 2016;7(2):163-169.
26. Ghasemi Hamidabadi H, Rezvani Z, Nazm Bojnordi M, et al. Chitosan-intercalated montmorillonite/poly (vinyl alcohol) nanofibers as a platform to guide neuronlike differentiation of human dental pulp stem cells. *ACS Appl Mater Interfaces*. 2017;9(13):11392-11404.

27. Poursamar SA, Azami M, Mozafari M. Controllable synthesis and characterization of porous polyvinyl alcohol/hydroxyapatite nanocomposite scaffolds via an in situ colloidal technique. *Colloids Surf B Biointerfaces*. 2011;84(2):310-316.
28. Stocco E, Barbon S, Lora L, et al. Partially oxidized polyvinyl alcohol conduitfor peripheral nerve regeneration. *Sci Rep*. 2018;8(1):604.
29. Wang C, Zhao M, Li J, et al. Silver nanoparticles/graphene oxide decorated carbon fiber synergistic reinforcement in epoxy-based composites. *Polymer*. 2017;131:263-271.
30. Nonahal M, Rastin H, Saeb MR, et al. Epoxy/PAMAM dendrimer-modified graphene oxide nanocomposite coatings: nonisothermal cure kinetics study. *Prog Org Coat*. 2018;114:233-243.
31. He Y, Yang S, Liu H, et al. Reinforced carbon fiber laminates with oriented carbon nanotube epoxy nanocomposites: magnetic field assisted alignment and cryogenic temperature mechanical properties. *J Colloid Interface Sci*. 2018;517:40-51.
32. Zhao M, Meng L, Ma L, et al. Layer-by-layer grafting CNTs onto carbon fibers surface for enhancing the interfacial properties of epoxy resin composites. *Compos Sci Technol*. 2018;154:28-36.
33. Wu Z, Gao S, Chen L, et al. Electrically insulated epoxy nanocomposites reinforced with synergistic core–shell SiO2@ MWCNTs and montmorillonite bifillers. *Macromol Chem Phys*. 2017;218(23):1700357.
34. Song B, Wang T, Sun H, et al. Graphitic carbon nitride (g-C3N4) interfacially strengthened carbon fiber epoxy composites. *Compos SciTechnol*. 2018;167:515-521.
35. Hu Z, Zhang D, Lu F, et al. Multistimuli-responsive intrinsic self-healing epoxy resin constructed by host–guest interactions. *Macromolecules*. 2018;51(14):5294-5303.
36. Zhang Y, Zhao M, Zhang J, et al. Excellent corrosion protection performance of epoxy composite coatings filled with silane functionalized silicon nitride. *J Polymer Res*. 2018;25(5):130.
37. Liu Z, Liu X, Zheng G, et al. Mechanical enhancement of melt-stretched β-nucleated isotactic polypropylene: the role of lamellar branching of β-crystal. *Polymer Test*. 2017;58:227-235.
38. Jiang J, Liu X, Lian M, et al. Self-reinforcing and toughening isotactic polypropylene via melt sequential injection molding. *Polymer Testing*. 2018;67:183-189.
39. Kong Y, Li Y, Hu G, et al. Preparation of polystyrene-b-poly (ethylene/propylene)-b-polystyrene grafted glycidyl methacrylate and its compatibility with recycled polypropylene/recycled high impact polystyrene blends. *Polymer*. 2018;145:232-241.
40. Zhang X, Wang X, Liu X, et al. Porous polyethylene bundles with enhanced hydrophobicity and pumping oil-recovery ability via skin-peeling. *ACS Sustain Chem Eng*. 2018;6(10):12580-12585.
41. Kong Y, Li Y, Hu G, et al. Effects of polystyrene-b-poly (ethylene/propylene)-b-polystyrene compatibilizer on the recycled polypropylene and recycled high-impact polystyrene blends. *Polym Adv Technol*. 2018;29(8):2344-2351.
42. Cui X, Zhu G, Pan Y, et al. Polydimethylsiloxane-titania nanocomposite coating: fabrication and corrosion resistance. *Polymer*. 2018; 138:203-210.
43. Sun K, Xie P, Wang Z, et al. Flexible polydimethylsiloxane/multi-walled carbon nanotubes membranous metacomposites with negative permittivity. *Polymer*. 2017;125:50-57.
44. Xu M, Ma K, Jiang D, et al. Hexa-[4-(glycidyloxycarbonyl) phenoxy] cyclotriphosphazene chain extender for preparing high-performance flame retardant polyamide 6 composites. *Polymer*. 2018;146:63-72.
45. Ding W, Wei S, Zhu J, Chen X, Rutman D, Guo Z. Manipulated electrospun PVA nanofibers with inexpensive salts. *Macromol Mater Eng*. 2010;295(10):958-965.
46. Suo B, Su X, Wu J, Chen D, Wang A, Guo Z. Poly (vinyl alcohol) thin film filled with CdSe–ZnS quantum dots: fabrication, characterization and optical properties. *Mater Chem Phys*. 2010;119(1–2):237-242.
47. Karbassi M, Zarrintaj P, Ghafarinazari A, et al. Microemulsion-based synthesis of a visible-light-responsive Si-doped TiO2 photocatalyst and its photodegradation efficiency potential. *Mater Chem Phys*. 2018;220:374-382.
48. Zarrintaj P, Mostafapoor F, Milan P, Saeb M. Theranostic platforms proposed for cancerous stem cells: a review. *Curr Stem Cell Res Ther*. 2018;13:1-9.
49. Derakhshandeh MR, Eshraghi MJ, Hadavi MM, et al. Diamond-like carbon thin films prepared by pulsed-DC PE-CVD for biomedical applications. *Surface Innovations*. 2018;6(3):167-175.
50. Li Y, Jing T, Xu G, et al. 3-D magnetic graphene oxide-magnetite poly (vinyl alcohol) nanocomposite substrates for immobilizing enzyme. *Polymer*. 2018;149:13-22.
51. Yang W, Fortunati E, Bertoglio F, et al. Polyvinyl alcohol/chitosan hydrogels with enhanced antioxidant and antibacterial properties induced by lignin nanoparticles. *Carbohydr Polym*. 2018;181:275-284.
52. Habiba U, Siddique TA, Lee JJL, Joo TC, Ang BC, Afifi AM. Adsorption study of methyl orange by chitosan/polyvinyl alcohol/zeolite electrospun composite nanofibrous membrane. *Carbohydr Polym*. 2018;191:79-85.
53. Noshirvani N, Hong W, Ghanbarzadeh B, Fasihi H, Montazami R. Study of cellulose nanocrystal doped starch-polyvinyl alcohol bionanocomposite films. *Int J Biol Macromol*. 2018;107:2065-2074.
54. Khorasani MT, Joorabloo A, Moghaddam A, Shamsi H, MansooriMoghadam Z. Incorporation of ZnO nanoparticles into heparinised polyvinyl alcohol/chitosan hydrogels for wound dressing application. *Int J Biol Macromol*. 2018;114:1203-1215.
55. Du H, Zhao CX, Lin J, et al. Carbon nanomaterials in direct liquid fuel cells. *Chem Rec*. 2018;18(9):1365-1372.
56. Zhang Y, Qian L, Zhao W, et al. Highly efficient Fe-NC nanoparticles modified porous graphene composites for oxygen reduction reaction. *J Electrochem Soc*. 2018;165(9):H510-H516.
57. Wang Z, Wei R, Gu J, et al. Ultralight, highly compressible and fire-retardant graphene aerogel with self-adjustable electromagnetic wave absorption. *Carbon*. 2018;139:1126-1135.
58. Gong K, Guo S, Zhao Y, et al. Bacteria cell templated porous polyaniline facilitated detoxification and recovery of hexavalent chromium. *J Mater Chem A*. 2018;6(35):16824-16832.
59. Guo J, Song H, Liu H, et al. Polypyrrole-interface-functionalized nano-magnetite epoxy nanocomposites as electromagnetic wave absorbers with enhanced flame retardancy. *J Mater Chem C*. 2017;5(22): 5334-5344.
60. Nourani-Vatani M, Ganjali M, Solati-Hashtjin M, Zarrintaj P, Saeb MR. Zirconium-based hybrid coatings: a versatile strategy for biomedical engineering applications. *Mater Today Proc*. 2018;5(7):15524-15531.
61. Nemati A, Saghafi M, Khamseh S, Alibakhshi E, Zarrintaj P, Saeb MR. Magnetron-sputtered Ti x N y thin films applied on titanium-based alloys for biomedical applications: composition-microstructure-property relationships. *Surf Coat Technol*. 2018;349:251-259.
62. Dong M, Li Q, Liu H, et al. Thermoplastic polyurethane-carbon black nanocomposite coating: fabrication and solid particle erosion resistance. *Polymer*. 2018;158:381-390.
63. Wang C, Murugadoss V, Kong J, et al. Overview of carbon nanostructures and nanocomposites for electromagnetic wave shielding. *Carbon*. 2018;140:696-733.

64. Su T, Shao Q, Qin Z, Guo Z, Wu Z. Role of interfaces in two-dimensional photocatalyst for water splitting. *ACS Catal*. 2018;8(3):2253-2276.
65. Zhang L, Zhang Q, Xie H, et al. Electrospun titania nanofibers segregated by graphene oxide for improved visible light photocatalysis. *Appl Catal Environ*. 2017;201:470-478.
66. Lin C, Hu L, Cheng C, et al. Nano-TiNb2O7/carbon nanotubes composite anode for enhanced lithium-ion storage. *Electrochim Acta*. 2018;260:65-72.
67. Tian J, Shao Q, Dong X, et al. Bio-template synthesized NiO/C hollow microspheres with enhanced Li-ion battery electrochemical performance. *Electrochim Acta*. 2018;261:236-245.
68. Pan F, Xiang X, Li Y. Nitrogen coordinated single atomic metals supported on Nanocarbons: a new frontier in Electrocatalytic CO2 reduction. *Engineered Sci*. 2018;1:12.
69. Cheng C, Fan R, Wang Z, et al. Tunable and weakly negative permittivity in carbon/silicon nitride composites with different carbonizing temperatures. *Carbon*. 2017;125:103-112.
70. Wu N, Liu C, Xu D, et al. Enhanced electromagnetic wave absorption of three-dimensional porous Fe3O4/C composite flowers. *ACS Sustainable Chem Eng*. 2018;6(9):12471-12480.
71. Hafshejani TM, Zamanian A, Venugopal JR, et al. Antibacterial glass-ionomer cement restorative materials: a critical review on the current status of extended release formulations. *J Control Release*. 2017;262:317-328.
72. Derakhshandeh MR, Eshraghi MJ, Javaheri M, et al. Diamond-like carbon-deposited films: a new class of biocorrosion protective coatings. *Surface Innov*. 2018;1-11.
73. Sadeghi-Kiakhani M, Khamseh S, Rafie A, Tekieh SMF, Zarrintaj P, Saeb MR. Thermally stable antibacterial wool fabrics surface-decorated by TiON and TiON/cu thin films. *Surface Innov*. 2018;6:258-265.
74. Guo B, Ma PX. Conducting polymers for tissue engineering. *Biomacromolecules*. 2018;19(6):1764-1782.
75. Zarrintaj P, Ahmadi Z, Vahabi H, Ducos F, Saeb MR, Mozafari M. Polyaniline in retrospect and prospect. *Mater Today: Proc*. 2018;5(7):15852-15860.
76. Guo B, Glavas L, Albertsson A-C. Biodegradable and electrically conducting polymers for biomedical applications. *Prog Polym Sci*. 2013;38(9):1263-1286.
77. Zarrintaj P, Bakhshandeh B, Saeb MR, et al. Oligoaniline-based conductive biomaterials for tissue engineering. *Acta Biomater*. 2018;72:16-34.
78. Mohammadi Amirabad L, Massumi M, Shamsara M, et al. Enhanced cardiac differentiation of human cardiovascular disease patient-specific induced pluripotent stem cells by applying unidirectional electrical pulses using aligned electroactive nanofibrous scaffolds. *ACS Appl Mater Interfaces*. 2017;9(8):6849-6864.
79. Amari A, Ebtekar M, Moazzeni S, et al. In vitro generation of IL-35-expressing human Wharton's jelly-derived mesenchymal stem cells using lentiviral vector. *Iran J Allergy Asthma Immunol*. 2015;14(4):416-426.
80. Zarrintaj P, Bakhshandeh B, Rezaeian I, Heshmatian B, Ganjali MR. A Novel electroactive agarose-aniline Pentamer platform as a potential candidate for neural tissue engineering. *Sci Rep*. 2017;7(1):17187.
81. Zarrintaj P, Rezaeian I, Bakhshandeh B, Heshmatian B, Ganjali MR. Bioconductive scaffold based on agarose-polyaniline for tissue engineering. *J Skin Stem Cell*. 2017;4(2):67394-67396.
82. Atoufi Z, Zarrintaj P, Motlagh GH, Amiri A, Bagher Z, Kamrava SK. A novel bio electro active alginate-aniline tetramer/agarose scaffold for tissue engineering: synthesis, characterization, drug release and cell culture study. *J Biomater Sci Polym Ed*. 2017;28(15):1617-1638.
83. Zarrintaj P, Urbanska AM, Gholizadeh SS, Goodarzi V, Saeb MR, Mozafari M. A facile route to the synthesis of anilinic electroactive colloidal hydrogels for neural tissue engineering applications. *J Colloid Interface Sci*. 2018;516:57-66.
84. Chen J, Yu M, Guo B, Ma PX, Yin Z. Conductive nanofibrous composite scaffolds based on in-situ formed polyaniline nanoparticle and polylactide for bone regeneration. *J Colloid Interface Sci*. 2018;514:517-527.
85. Fernandes EG, Zucolotto V, De Queiroz AA. Electrospinning of hyperbranched poly-l-lysine/polyaniline nanofibers for application in cardiac tissue engineering. *J Macromol Sci, Part A: Pure Appl Chem*. 2010;47(12):1203-1207.
86. Zamanlui S, Amirabad LM, Soleimani M, Faghihi S. Influence of hydrodynamic pressure on chondrogenic differentiation of human bone marrow mesenchymal stem cells cultured in perfusion system. *Biologicals*. 2018;56:1-8.
87. Amari A, Ebtekar M, Moazzeni SM, et al. Investigation of immunomodulatory properties of human Wharton's jelly-derived mesenchymal stem cells after lentiviral transduction. *Cell Immunol*. 2015;293(2):59-66.
88. Dodel M, Nejad NH, Bahrami SH, et al. Electrical stimulation of somatic human stem cells mediated by composite containing conductive nanofibers for ligament regeneration. *Biologicals*. 2017;46:99-107.
89. Baheiraei N, Yeganeh H, Ai J, et al. Preparation of a porous conductive scaffold from aniline pentamer-modified polyurethane/PCL blend for cardiac tissue engineering. *J Biomed Mater Res A*. 2015;103(10):3179-3187.
90. Baheiraei N, Gharibi R, Yeganeh H, et al. Electroactive polyurethane/siloxane derived from castor oil as a versatile cardiac patch, part II: HL-1 cytocompatibility and electrical characterizations. *J Biomed Mater Res A*. 2016;104(6):1398-1407.
91. Niple J, Daigle J, Zaffanella L, Sullivan T, Kavet R. A portable meter for measuring low frequency currents in the human body. *Bioelectromagnetics: J Bioelectromagnetics Soc, Soc Phys Regul Biol Med, Eur Bioelectromagnetics Assoc*. 2004;25(5):369-373.
92. Liu Y, Cui H, Zhuang X, Wei Y, Chen X. Electrospinning of aniline pentamer-graft-gelatin/PLLA nanofibers for bone tissue engineering. *Acta Biomater*. 2014;10(12):5074-5080.
93. Liu Y, Geever LM, Kennedy JE, Higginbotham CL, Cahill PA, McGuinness GB. Thermal behavior and mechanical properties of physically crosslinked PVA/gelatin hydrogels. *J Mech Behav Biomed Mater*. 2010;3(2):203-209.
94. Wang M, Li Y, Wu J, Xu F, Zuo Y, Jansen J. In vitro and in vivo study to the biocompatibility and biodegradation of hydroxyapatite/poly (vinyl alcohol)/gelatin composite. *J Biomed Mater Res Part A: Off J Soc Biomater, Jpn Soc Biomater, Aust Soc Biomater Korean Soc Biomater*. 2008;85(2):418-426.
95. Yang D, Li Y, Nie J. Preparation of gelatin/PVA nanofibers and their potential application in controlled release of drugs. *Carbohydr Polym*. 2007;69(3):538-543.
96. Kim H, Jeong S-M, Park J-W. Electrical switching between vesicles and micelles via redox-responsive self-assembly of amphiphilic rod− coils. *J Am Chem Soc*. 2011;133(14):5206-5209.

How to cite this article: Shojaie S, Rostamian M, Samadi A, et al. Electrospun electroactive nanofibers of gelatin-oligoaniline/Poly (vinyl alcohol) templates for architecting of cardiac tissue with on-demand drug release. *Polym Adv Technol*. 2019;1-11. https://doi.org/10.1002/pat.4579